

Suppression of Channel Shortening and Reduction of S/D Parasitic Resistance in InGaZnO channel BEOL Transistor by Insertion of thermally stable InAlZnO Contact Layer

Yuta Sato, Hirokazu Fujiwara, Nobuyoshi Saito, Tomomasa Ueda, and Keiji Ikeda
Institute of Memory Technology Research & Development, Kioxia Corporation,
Email: yuta6.sato@kioxia.com

Abstract

We have demonstrated a suppression of channel shortening and a reduction of S/D parasitic resistance (R_{para}) in InGaZnO (IGZO)-FET after high temperature annealing by inserting InAlZnO (IAZO) contact layer (CL) between S/D electrode and channel. Thanks to high bond dissociation energy of Al with oxygen, tungsten (W) film covered by IAZO maintained a low resistivity during high temperature annealing ($>400^\circ\text{C}$), while W film covered by IGZO significantly increased its resistivity due to the formation of metal oxide interlayer. IGZO-FET with IAZO-CL shows both improvement of V_{th} roll-off and reduction of R_{para} by $\sim 30\%$, with maintaining high mobility ($>15 \text{ cm}^2/\text{Vs}$) even after 420°C annealing in N_2 . The insertion of IAZO contact layer is a promising technique to achieve IGZO-channel BEOL transistor with high thermal stability and high on-current.

(Keywords: oxide semiconductor, InGaZnO, InAlZnO)

Introduction

Field-effect-transistor (FET) using oxide semiconductors (OS) as channel layers have attracted much attention as BEOL transistor for 3D-LSI applications such as high voltage I/Os and embedded memory by its high mobility ($>10 \text{ cm}^2/\text{Vs}$), high breakdown voltage ($V_{\text{BD}} > 40\text{V}$) and ultralow leakage current ($<10^{-22} \text{ A}/\mu\text{m}$) [1-5]. For integrating OS-FET in BEOL of Si CMOS LSI, oxidation/deoxidation between OS channel and S/D electrode during thermal process ($> 350^\circ\text{C}$) causes two fatal issues especially for scaling beyond $1 \mu\text{m}$ gate length region as shown in Fig.1 (a); (1) a channel shortening caused by extension of N^+ S/D region by the formation of oxygen vacancy (V_{o}) which generates excess carriers and (2) an increase of S/D parasitic resistance (R_{para}) by the formation of highly resistive oxide interface layer of S/D electrode [6-9]. In order to overcome these issues, we focused on a thermally stable OS material, InAlZnO (IAZO). Since Al-O exhibits much larger bond dissociation energy than Ga-O, IAZO is expected to suppress oxidation/deoxidation with S/D electrode, compared with IGZO [10,11]. We propose an insertion of IAZO as a contact layer (IAZO-CL) between S/D electrode and IGZO channel as shown in Fig. 1(b). In this study, we have successfully demonstrated suppression of channel shortening and R_{para} in IGZO-FET by applying IAZO-CL with maintaining high mobility ($>15 \text{ cm}^2/\text{Vs}$) of IGZO channel.

Results and Discussion

A. Thermal stability of IAZO-CL

Figure 2 shows four different chemical compositions of IAZO film and their sheet resistances. In Al-rich condition, deposited IAZO film behaved as an insulator. With the decrease of Al composition, the resistivity of IAZO film decreased. Thus, IAZO film in condition 4 (IAZO-4) was expected as a contact layer with low resistivity. Figure 3 shows the O 1s XPS spectra of IAZO and IGZO film. The O1s spectra were deconvoluted into two different peaks, where one is the peak related to metal-O at 530.85 eV and the other is the peak related to oxygen vacancy at 532.10 eV [12, 13]. Smaller peak area in IAZO film indicates Al suppresses V_{o} formation compared with Ga. In order to investigate the degree of oxidation/deoxidation between S/D electrode and OS channel, the sheet resistance of tungsten (W) film covered by different OS materials were evaluated (Fig.4). The thickness of W and OS film were 10 nm both. In this experiment for

IAZO, condition 4 in Fig.2 was used. The resistance of OS/W film corresponded to that of W film during annealing ($<380^\circ\text{C}$). As annealing temperature increases ($>400^\circ\text{C}$), the resistivity of W covered by IGZO was increased drastically, while that of W covered by IAZO was maintained. It suggests that IAZO film suppresses oxidation/deoxidation with S/D electrode (W) and the formation of highly resistive metal oxide interlayer.

B. Characterization of IGZO-FET with IAZO-CL

Figure 5 shows device fabrication process and schematic illustration of IGZO-FET. The thickness of gate insulator, IGZO channel and IAZO-CL were 40 nm , 15 nm and 5 nm , respectively. Tungsten was used as S/D electrodes. Fig. 6 shows $I_{\text{d}}-V_{\text{g}}$ characteristics of IGZO-FET with (w/) and without (w/o) IAZO-CL, after annealing at 420°C under N_2 atmosphere. S.S. value of IGZO-FET w/o IAZO was deteriorated compared with that w/ IAZO-CL. This S.S. degradation was due to the shortening of effective channel length in IGZO-FET w/o IAZO-CL. In addition, the increase of drain current by 7% was achieved with IAZO-CL. The comparison of $R_{\text{on}}-L_{\text{g}}$ plot in both devices is shown in Fig. 7(a). R_{para} was extracted by the vertical intersection point of $R_{\text{on}}-L_{\text{g}}$ plot and extracted R_{para} are shown in Fig. 7(b). R_{para} of IGZO-FET w/ IAZO-CL was confirmed to decrease by 30% , compared with that of IGZO-FET w/o IAZO-CL. This R_{para} reduction is caused by suppression of S/D electrode oxidation by IAZO-CL. Figure 8 shows effective mobility extracted by split $C-V$ method. Comparable high mobility ($>15 \text{ cm}^2/\text{Vs}$) was confirmed in IGZO-FET w/ IAZO-CL. Figure 9 shows the threshold voltage shift (ΔV_{th}) plotted versus L_{g} , where ΔV_{th} is defined as the difference of V_{th} from V_{th} of $L_{\text{g}}=2 \mu\text{m}$. IGZO-FET w/ IAZO-CL maintained V_{th} even at shorter L_{g} ($L_{\text{g}} < 1 \mu\text{m}$), while clear V_{th} drop was observed in IGZO-FET w/o IAZO-CL. This indicates that IAZO-CL has high immunity to deoxidation by S/D metal and suppresses extension of N^+ S/D region toward IGZO channel. Moreover, it was revealed that only 5 nm contact layer played an important role for improving thermal stability of OS-FET without changing the channel material. Figure 10 shows the $I_{\text{on}}-L_{\text{g}}$ plot of experimental results and calculated value from extracted mobility and R_{para} . The calculated on-current would increase by 40% at $L_{\text{g}}=100 \text{ nm}$ w/ IAZO-CL thanks to low R_{para} .

Conclusion

We have successfully demonstrated improvement of thermal stability of IGZO-FET by inserting IAZO contact layer between IGZO channel and S/D electrode. The IAZO contact layer has high immunity to deoxidation of channel by S/D metal and suppresses oxidation of S/D metal during thermal process. By inserting IAZO contact layer to IGZO-FET, V_{th} roll-off was improved and R_{para} was decreased by 30% with maintaining high mobility ($>15 \text{ cm}^2/\text{Vs}$). These results indicate that IAZO contact layer is promising to realize short channel IGZO-FET for 3D-LSI applications.

References

- [1] S. -J. Choi *et al.*, IEICE Electronics Express, 16, 3(2019), [2] K. Nomura *et al.*, Nature, 432,488(2004), [3] K. Kaneko *et al.*, VLSI 2011, p120, [4] T. Aoki *et al.*, ISSCC 2014, p502, [5] S. H. Wu *et al.*, VLSI 2016, p58, [6] M. Oota *et al.*, IEDM 2019 p.50, [7] J. Kataoka *et al.*, JJAP, 58, SBBJ03 (2019), [8] K.-H. Choi *et al.*, Appl. Phys. Lett. 102, 052103 (2013), [9] Z. Hu *et al.*, Solid-State Electronics. 104, 39–43(2014), [10] H. Fujiwara *et al.*, VLSI2020, T-H2-2 [11] Y. R. Luo, Handbook of Chemistry and Physics, CRC Press, 2007, [12] Jie Zhang *et al.*, J. Vac. Sci. Technol. B 32,1 (2014), [13] Lan Yue *et al.*, J. Phys. D: Appl. Phys. 46,445106(2013)

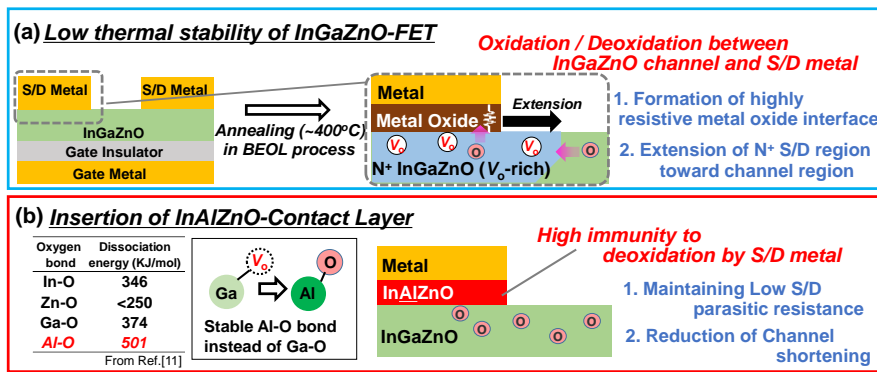


Fig. 1 (a) Schematic illustration of issues in IGZO-channel FET for high-temperature annealing, and (b) list of metal-oxygen bond dissociation energy [11] and concepts of a reduction of S/D parasitic resistance and a suppression of channel shortening by IAZO-contact layer.

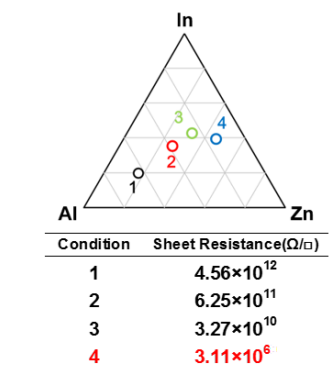


Fig. 2 Chemical composition and sheet resistance of deposited IAZO films. IAZO film with less Al composition shows a lower resistivity.

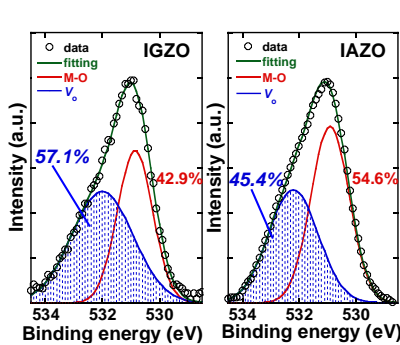


Fig. 3 XPS spectra of O1s in IGZO and IAZO film. The peak area of V_O in IAZO film is smaller than that in IGZO film.

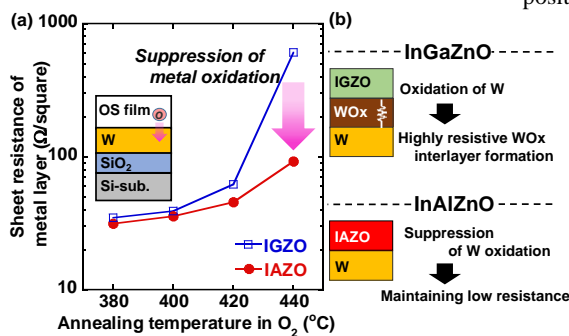


Fig. 4 (a) Annealing temperature dependence of sheet resistance of tungsten film covered by OS materials and (b) schematic diagram of comparison between IGZO and IAZO.

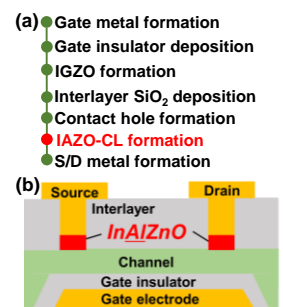


Fig. 5 (a) Fabrication process and (b) schematic image of IGZO-FET w/ IAZO-CL.

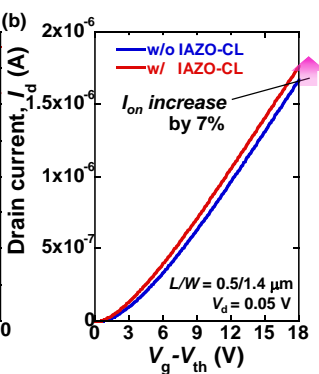
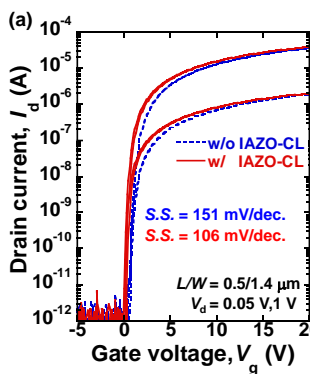


Fig. 6 I_d - V_g characteristics of IGZO-FET w/ and w/o IAZO-CL after annealing at $420^{\circ}C$ under N_2 atmosphere. Drain current of IGZO FET w/ IAZO-CL was increased by 7%.

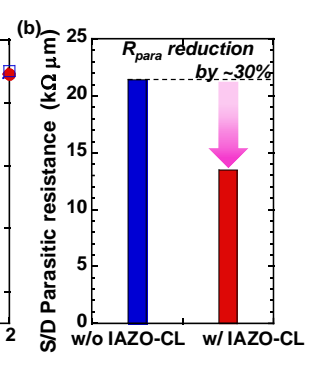
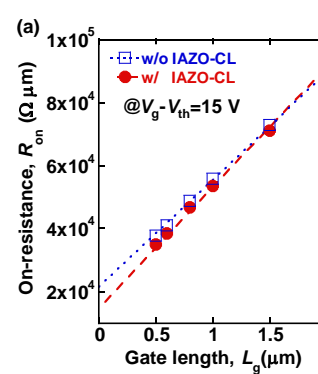


Fig. 7 (a) R_{on} - L_g plot and (b) comparison of R_{para} between IGZO-FET w/ and w/o IAZO-CL. R_{para} is decreased by 30% by the insertion of IAZO-CL.

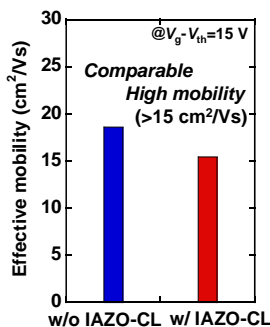


Fig. 8 Effective mobility extracted by split C-V method. High mobility (>15 cm^2/Vs) was maintained.

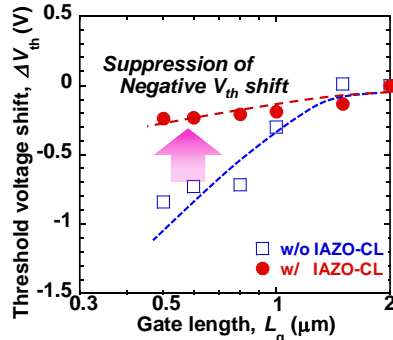


Fig. 9 ΔV_{th} roll-off curve after annealing at $420^{\circ}C$ under N_2 atmosphere. Negative shift of V_{th} was reduced by insertion of IAZO-CL.

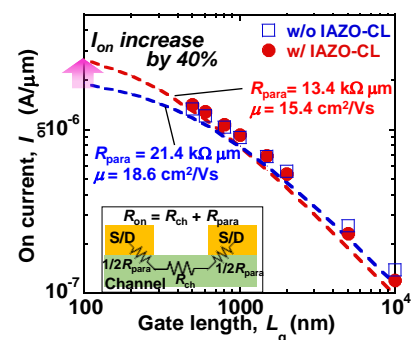


Fig. 10 I_{on} improvement by L_g scaling calculated from extracted mobility and R_{para} . I_{on} is expected to increase by 40% with IAZO-CL at $L_g = 100$ nm.